Virologica Sinica (2021) 36:981–996
https://doi.org/10.1007/s12250-021-00351-5

www.virosin.org
www.springer.com/12250

RESEARCH ARTICLE

Role of Intracellular Distribution of Feline and Bovine SAMHD1 Proteins in Lentiviral Restriction

Chu Wang[1,2] · Lina Meng[1] · Jialin Wang[1] · Kaikai Zhang[1] · Sizhu Duan[1] · Pengyu Ren[1] · Yingzhe Wei[1] · Xinyu Fu[1] · Bin Yu[1,3] · Jiaxin Wu[1,3] · Xianghui Yu[1,3]

Received: 3 August 2020 / Accepted: 28 December 2020 / Published online: 22 March 2021

Abstract

Human SAMHD1 (hSAM) restricts lentiviruses at the reverse transcription step through its dNTP triphosphohydrolase (dNTPase) activity. Besides humans, several mammalian species such as cats and cows that carry their own lentiviruses also express SAMHD1. However, the intracellular distribution of feline and bovine SAMHD1 (fSAM and bSAM) and its significance in their lentiviral restriction function is not known. Here, we demonstrated that fSAM and bSAM were both predominantly localized to the nucleus and nuclear localization signal (^{11}KRPR^{14})-deleted fSAM and bSAM relocalized to the cytoplasm. Both cytoplasmic fSAM and bSAM retained the antiviral function against different lentiviruses and cytoplasmic fSAM could restrict Vpx-encoding SIV and HIV-2 more efficiently than its wild-type (WT) protein as cytoplasmic hSAM. Further investigation revealed that cytoplasmic fSAM was resistant to Vpx-induced degradation like cytoplasmic hSAM, while cytoplasmic bSAM was not, but they all demonstrated the same *in vitro* dNTPase activity and all could interact with Vpx as their WT proteins, indicating that cytoplasmic hSAM and fSAM can suppress more SIV and HIV-2 by being less sensitive to Vpx-mediated degradation. Our results suggested that fSAM- and bSAM-mediated lentiviral restriction does not require their nuclear localization and that fSAM shares more common features with hSAM. These findings may provide insights for the establishment of alternative animal models to study SAMHD1 *in vivo*.

Keywords SAMHD1 · Feline SAMHD1 (fSAM) · Bovine SAMHD1 (bSAM) · Nuclear localization signal (NLS) · Vpx · Degradation · Viral restriction

Introduction

SAM domain and HD domain-containing protein 1 (SAMHD1) is an antiviral dNTP triphosphohydrolase (dNTPase) that suppresses lentiviral replication by reducing the concentration of cellular dNTPs to a level insufficient for viral cDNA synthesis (Goldstone *et al.* 2011; Powell *et al.* 2011; Kim *et al.* 2012; Lahouassa *et al.* 2012; St Gelais *et al.* 2012). However, lowering cellular dNTP levels may not be the sole mechanism of restriction (White *et al.* 2013b; Bhattacharya *et al.* 2016; Welbourn and Strebel 2016). Activation of the dNTPase activity of SAMHD1 relies on its catalytically-active tetrameric state initiated by GTP/dGTP binding (Amie *et al.* 2013; Ji *et al.* 2013, 2014; Koharudin *et al.* 2014; Zhu *et al.* 2015). Phosphorylation of SAMHD1 by cyclin-dependent kinases at the Thr 592 residue reduces the stability of the SAMHD1 tetramer, leading to the loss of antiviral activity of SAMHD1 (Cribier *et al.* 2013; White *et al.* 2013b; Pauls

Chu Wang and Lina Meng have contributed equally to this work.

Electronic supplementary material The online version of this article (https://doi.org/10.1007/s12250-021-00351-5) contains supplementary material, which is available to authorized users.

✉ Xianghui Yu
xianghui@jlu.edu.cn

✉ Jiaxin Wu
wujiaxin@jlu.edu.cn

[1] National Engineering Laboratory for AIDS Vaccine, School of Life Sciences, Jilin University, Changchun 130012, China

[2] The First Hospital and Institute of Immunology, Jilin University, Changchun 130012, China

[3] Key Laboratory for Molecular Enzymology and Engineering, the Ministry of Education, School of Life Sciences, Jilin University, Changchun 130012, China

et al. 2014; Tang *et al.* 2015; Yan *et al.* 2015). As counter mechanisms, viral protein X (Vpx) from human immunodeficiency virus type 2 (HIV-2) and some strains of simian immunodeficiency virus (SIV) recruits SAMHD1 to the E3 ubiquitin ligase complex $CRL4^{DCAF1}$ for ubiquitination (Srivastava *et al.* 2008; Bergamaschi *et al.* 2009; Hrecka *et al.* 2011; Laguette *et al.* 2011; Ahn *et al.* 2012). This recruitment leads to proteasomal degradation of SAMHD1, which elevates cellular dNTP concentration and, therefore, relieves SAMHD1-mediated restriction of lentiviral replication in monocyte/macrophages and resting T cells (Hrecka *et al.* 2011; Laguette *et al.* 2011; Ahn *et al.* 2012; Baldauf *et al.* 2012; Berger *et al.* 2012; Descours *et al.* 2012). HIV-1 lacks a Vpx protein and its viral protein R (Vpr) cannot mediate the proteasomal degradation of SAMHD1, although some other SIV strains employ the related Vpr protein to fulfill the same function (Lim *et al.* 2012; Spragg and Emerman 2013). In addition to primate lentiviruses, SAMHD1 also has been shown to restrict a variety of other retroviruses and DNA and other RNA viruses, such as feline immunodeficiency virus (FIV), bovine immunodeficiency virus (BIV), hepatitis B virus and enterovirus 71 (Gramberg *et al.* 2013; Hollenbaugh *et al.* 2013; Kim *et al.* 2013; White *et al.* 2013a; Chen *et al.* 2014; Li *et al.* 2020).

Wild-type (WT) human SAMHD1 (hSAM) is predominantly localized to the nucleus, which is mediated by a nuclear localization signal (NLS) in the N-terminus of SAMHD1. Disruption of the NLS results in cytoplasmic accumulation of the SAMHD1 protein and renders it resistant to Vpx-induced degradation (Brandariz-Nunez *et al.* 2012; Hofmann *et al.* 2012; Wei *et al.* 2012). However, cytoplasmic hSAM still interacts with Vpx, maintains dNTPase activity and inhibits lentiviral infection, suggesting that the intracellular dNTPs can freely diffuse throughout the cell (Brandariz-Nunez *et al.* 2012; Hofmann *et al.* 2012). Many SAMHD1 mutations found in patients with Aicardi-Goutières syndrome (AGS) can also disrupt nuclear localization, leading to SAMHD1 accumulation in the cytoplasm (Rice *et al.* 2009; Goncalves *et al.* 2012; White *et al.* 2017).

Feline SAMHD1 (fSAM) and bovine SAMHD1 (bSAM) could restrict their host species-carrying lentiviruses FIV and BIV, respectively, by using their dNTPase activities (Mereby *et al.* 2018). To facilitate the establishment of alternative animal models in addition to mice for investigating SAMHD1 *in vivo*, we previously studied the restriction profile of fSAM and bSAM against different primate lentiviruses and the molecular mechanisms of fSAM- and bSAM-mediated restriction (Wang *et al.* 2020). However, the intracellular distribution of fSAM and bSAM is not very clear, and the roles of intracellular distribution of fSAM and bSAM in cellular physiology and viral restriction are not well understood.

In this study, we first confirmed that the NLS sequence ^{11}KRPR^{14} was conserved in fSAM and bSAM and found that the NLS-deleted (NLS) fSAM and bSAM relocalized to the cytoplasm. Then we investigated the antiviral function of cytoplasmic fSAM and bSAM against different lentiviruses and found that cytoplasmic fSAM could restrict SIVmac239 and HIV-2 ROD more efficiently than its WT protein by being less sensitive to Vpx-mediated degradation like cytoplasmic hSAM. While cytoplasmic bSAM was different from cytoplasmic hSAM and fSAM in sensitivity to Vpx-mediated degradation, although it still retained the antiviral activity against different lentiviruses. These findings suggested that fSAM- and bSAM-mediated lentiviral restriction does not require their nuclear localization and that feline SAMHD1 shares more common features with human SAMHD1, thus is more suitable for the establishment of the animal model to study SAMHD1 *in vivo*.

Materials and Methods

Cell Lines and Cell Culture

HEK293, HEK293T and CrFK cells were purchased from the American Type Culture Collection (ATCC, Manassas, VA, USA). TZM-bl and U937 cells were provided by the National Institutes of Health-AIDS Reagent Program (NIH-ARP). HEK293, HEK293T, TZM-bl and CrFK cells were maintained in Dulbecco's modified Eagle's medium (DMEM) supplemented with 10% fetal bovine serum (FBS). Stable U937 cells were maintained in RPMI 1640 medium with 10% FBS and 1 μg/mL puromycin and were differentiated with PMA (phorbol 12-myristate 13-acetate; 25 ng/mL) for 20 h before use. All cell lines were cultured at 37 °C and 5% CO_2.

Plasmids

Plasmids pVR1012-homo-SAMHD1-HA, pCG-Vpx_{mac}-HA, and pCG-$Vpx_{mac/Q76A}$-HA were gifts from Dr. Wenyan Zhang (Institute of Virology and AIDS Research, First Hospital of Jilin University). pVR1012-feline-SAMHD1-HA, pVR1012-bovine-SAMHD1-HA, pVR1012-Vpx_{mac}-myc, pVR1012-Vpx_{ROD}-myc and pVR1012-$Vpx_{ROD/Q76A}$-myc were constructed as previously described (Wang *et al.* 2020). NLS-deleted human, feline and bovine SAMHD1 fragments with C-terminal hemagglutinin (HA) tags were generated by PCR using pVR1012-homo-SAMHD1-HA, pVR1012-feline-SAMHD1-HA and pVR1012-bovine-

SAMHD1-HA as templates, respectively. The 11–14 amino acids KRPR at the N-terminus of each species of SAMHD1 were deleted by using the following primers: for hSAM△NLS, forward primer: 5′-GCTCTAGAATGCAG CGAGCCGATTCCGAGCAGCCCTCCTGCGATGACA-3′; for fSAM△NLS, forward primer: 5′-GCTCTAGAATG CAGGGAGCAGACTCAGACCAGCCCTTCCGCGATG GCA-3′; for bSAM△NLS, forward primer: 5′-AAGTC-TAGAATGCAGAGTGCCGACTCCCAGAACACCCCC CGCGATGGCAGCCCAAGAAC-3′; the reverse primer for all three species of SAMHD1 was: 5′-CGGGATCCT-TACGCGTAATCTGGGACGTCGTAAGGG-3′. All PCR products were digested and cloned into the *Xba*I and *Bam*HI sites of pVR1012 vector. To construct enhanced green fluorescent protein (EGFP)-fused SAMHD1 proteins, the EGFP fragment was amplified from a plasmid pEGFP-N1 (Clontech, Mountain View, CA, USA) by using the forward primer: 5′-ACGCGTCGACATGGTGAGCAAGG GCG-3′ and reverse primer: 5′-GCTCTAGACTTGTA-CAGCTCGTCCATGC-3′. The PCR product was inserted into the WT and NLS-deleted SAMHD1-expressing plasmids at the *Sal*I and *Xba*I restriction sites. A plasmid pVR1012-EGFP expressing EGFP only was also constructed as a systemic control. HIV-2 ROD Vpx-expressing lentiviral backbone plasmid pLVX-Vpx_{ROD} was constructed by inserting the PCR-amplified Vpx fragment with a C-terminal FLAG tag into the *Xho*I and *Bam*HI sites of pLVX-puro vector.

Antibodies and Chemicals

Anti-HA mouse monoclonal antibody (mAb) (no. 901514) was purchased from Covance (Princeton, NJ, USA). Anti-myc mouse mAb (no. 05-419) was purchased from Millipore (Burlington, MA, USA). Anti-GAPDH mouse mAb (no. 60004-1-Ig) and anti-histone H3 mAb (no. 17168-1-AP) were purchased from Proteintech Group (Rosemont, IL, USA). Anti-SIV p27 mAb was provided by NIH-ARP. The proteasome inhibitor MG132 in DMSO solution (no. M7449) was purchased from Sigma-Aldrich (St. Louis, MO, USA). Alkaline phosphatase-conjugated goat anti-mouse IgG was obtained from Jackson Immunoresearch (Baltimore Pike, PA, USA).

Western Blotting

DNA transfection was carried out using jetPRIME transfection reagent (Polyplus transfection, Illkirch, France) according to the manufacturer's instructions. In co-transfection assays, cells were harvested at 48 h post-transfection, centrifuged at 3000 $\times g$ for 5 min and lysed with RIPA buffer (pH 7.4, containing 50 mmol/L Tris–HCl, 150 mmol/L NaCl, 1% Triton X-100, 1% sodium deoxycholate, 0.1% SDS, and 1 mmol/L EDTA). For preparation of nuclear and cytoplasmic extracts, cell pellets harvested from 12-well plates were first resuspended in 80 μL of RLN buffer (pH 7.4, containing 50 mmol/L Tris–HCl, 40 mmol/L NaCl, 1.5 mmol/L $MgCl_2$, 0.5% Nonidet P-40) in the presence of protease inhibitor (Roche, South San Francisco, CA, USA) and incubated on ice for 5 min, and then centrifuged at 3000$\times g$ for 10 min at 4 °C to extract the supernatant as the cytoplasmic samples. The nuclear pellet was washed once with the RLN buffer and then resuspended in 20 μL of RIPA buffer. After vortexed for 30 min, the nuclear samples were centrifuged at 12,000 $\times g$ for 5 min at 4 °C to remove debris. In the SAMHD1 degradation assay with lentiviruses carrying Vpx, Lenti-Vpx_{ROD} pseudoviruses were produced by transfection into HEK293T cells with pLVX-Vpx_{ROD}, psPAX2 (Addgene, Watertown, MA, USA) and pVSV-G at a mass ratio of 1.6: 2: 1. The titer of Lenti-Vpx_{ROD} was determined by the concentration of p24 (Alliance HIV-1 P24 ANTIGEN ELISA Kit, PerkinElmer, Waltham, MA, USA). HEK293 cells (5×10^5) were infected with 3 μg p24 of Lenti-Vpx_{ROD} or incubated with DMEM supplemented with 10% FBS for 24 h, then transfected with 600 ng of different SAMHD1-HA expression plasmids or empty vector. Cells were harvested at 48 h post-transfection. All samples were mixed with 4× loading buffer and boiled at 97 °C for 10 min. The prepared protein samples were separated by electrophoresis on SDS–polyacrylamide gels (SDS–PAGE) and detected by immunoblotting as previously described (Wang *et al.* 2020).

Immunofluorescence Microscopy

HEK293 cells were seeded onto coverslips at 5×10^4 cells per well in 24-well plates one day before transfection. Cell monolayers were about 10%–20% confluence on the day of transfection. At 48 h post-transfection, monolayers were washed twice with phosphate buffered saline (PBS) and fixed with 4% paraformaldehyde in PBS for 15 min. Paraformaldehyde-fixed cells were then washed twice with PBS. Cellular nuclei were labeled with 1 μg/mL of DAPI (4′, 6-diamidino-2-phenylindole) in PBS for 5 min, then washed twice with PBS. Images were captured with a Confocal Laser Scanning Microscope (Zeiss, Oberkochen, Germany) using a 40× objective. For quantification of the percentage of nuclear SAMHD1 in WT and NLS-deleted SAMHD1 expressing cells, the average mean fluorescence intensity (MFI) per pixel of an area of interest in the nuclear and cytoplasmic areas were first determined using Adobe Photoshop (San Jose, CA, USA). Next, relative nuclear and cytoplasmic MFI was derived by subtracting the average background MFI from the average nuclear and cytoplasmic MFI, respectively, and sum of the relative

nuclear MFI and relative cytoplasmic MFI was calculated to represent the whole cell-associated SAMHD1. The percentage of nuclear SAMHD1 was then calculated as the ratio of the relative nuclear MFI to the sum MFI.

Viral Infectivity Assay

Viruses were generated by transfection into HEK293T cells. The infectious molecular clones for the generation of HIV-1 (NL4-3), SIVmac239 and HIV-2 ROD were provided by NIH-ARP. The FIV pseudovirus clone (pFP93 and pGINSIN) was described previously (Khare *et al.* 2008; Gramberg *et al.* 2013). The FIV-GFP reporter virus was produced by transfection with pFP93, pGINSIN and pVSV-G at a mass ratio of 3: 3: 1. The infectious titer of HIV-1, SIVmac239 and HIV-2 ROD was determined by the concentration of reverse transcriptase (RT) using a Lenti RT Activity Kit (Cavidi, Uppsala, Sweden). The titer of FIV-GFP was determined using HEK293T cells as the number of GFP-positive cells per mL of virus stock. The viral infectivity assay using TZM-bl cells was performed as previously described (Wang *et al.* 2020). Briefly, 2×10^5 TZM-bl cells transfected with SAMHD1 were infected with the RT concentration-determined viruses (0.1 ng RT of HIV-1, 1 ng RT of SIVmac239 or 1 ng RT of HIV-2 ROD) at 48 h post-transfection. The cells were fixed and stained with X-Gal (5-bromo-4-chloro-3-indolyl-β-d-galactopyranoside) at 48 h post-infection. The viral infectivity was determined by the number of positive blue cells. For the viral infectivity assay using HEK293T cells, cells transfected with or without SAMHD1 were detached with trypsin at 48 h post-transfection and were re-seeded into 24-well plates (2×10^5 cells per well) with FIV-GFP at multiplicities of infection (MOI) = 0.5. At 48 h post-infection, the cells were first observed under fluorescence microscope for GFP expression and then analyzed for the percentage of GFP-positive cells by flow cytometry. Each experiment was performed in triplicate.

Generation and Infection of Stable U937 Cell Lines

Stable U937 cells were generated and infected as previously described (Wang *et al.* 2020). Briefly, PMA-differentiated SAMHD1-expressing stable U937 cells (5×10^5) were infected with HIV-1 of 0.1 ng RT, SIVmac239 of 1 ng RT or HIV-2 ROD of 1 ng RT for 4 h, then washed three times with RPMI 1640 medium and cultured for 5 days to monitor the viral replication. The culture supernatants were harvested regularly to measure the concentration of p24 for HIV-1 or RT for SIVmac239 and HIV-2 ROD. For FIV-GFP, the PMA-differentiated cells (5×10^5) were infected with different amounts of the virus (MOI = 0.5, 1.0 or 2.0) and then analyzed for the percentage of GFP-positive cells at 48 h post-infection by flow cytometry. All infections were performed in triplicate.

In vitro dNTPase Activity Assay

The *in vitro* dNTPase activity assay was performed as previously described (Wang *et al.* 2020). Briefly, SAMHD1-transfected HEK293 cells in 12-well plates were harvested at 48 h post-transfection, washed twice with cold reaction buffer (pH 7.4, containing 50 mmol/L Tris–HCl, 50 mmol/L KCl and 5 mmol/L $MgCl_2$), and processed as described in the co-immunoprecipitation assay below. After incubated with anti-HA antibody-conjugated agarose beads (Roche) for 3 h, the beads were washed three times with washing buffer, once with reaction buffer and then resuspended in 40 μL reaction buffer. Partial bead slurry was reserved as the input control. The rest was diluted and incubated with 1 mmol/L dGTP and 0.01 U inorganic pyrophosphatase (New England Biolabs, Ipswich, MA, USA) at 37 °C for 2 h with occasional mixing. The reactions were stopped by heating to 70 °C for 5 min. The inorganic phosphate release from the reactions was measured using a Malachite Green Detection Kit (R&D Systems, Minneapolis, MN, USA) according to the manufacturer's instructions. All reactions were performed in triplicate.

Co-immunoprecipitation Assay

Cells in 6-well plates were harvested at 48 h post-transfection, washed twice with cold PBS and lysed in lysis buffer (pH 7.4, containing 50 mmol/L Tris–HCl, 150 mmol/L NaCl and 1% Triton X-100) supplemented with the protease inhibitor at 4 °C for 40 min. The cell lysates were centrifuged at 16,000×*g* for 15 min and the supernatants were incubated with anti-HA beads at 4 °C for 3 h. Then, the beads were washed three times with washing buffer (pH 7.4, containing 20 mmol/L Tris–HCl, 100 mmol/L NaCl and 0.05% Tween-20), resuspended with 2 × SDS sample buffer and boiled at 97 °C for 10 min. The prepared samples were subjected to SDS-PAGE and Immunoblotting.

Statistical Analysis

Data are shown as mean ± standard deviation (SD). Significance is calculated by using unpaired Student's *t*-test or repeated-measure analysis of two-way ANOVA with PRISM v6 (GraphPad Software, Inc., La Jolla, CA, USA). In all figures, * indicates $P \leq 0.05$, ** $P \leq 0.01$, and *** $P \leq 0.001$; *ns* indicates no significance.

Results

The NLS Sequence ^{11}KRPR^{14} Is Conserved in Feline and Bovine SAMHD1

Previous works have demonstrated that the NLS ^{11}KRPR^{14} of human SAMHD1 is required for its nuclear localization (Brandariz-Nunez *et al.* 2012; Hofmann *et al.* 2012). Alignment of amino acid sequences of the N-terminal domain of different SAMHD1 proteins demonstrated that ^{11}KRPR^{14} is conserved in the human, simian, feline and bovine homologues (Fig. 1A). To determine whether the ^{11}KRPR^{14} motif is also essential to the nuclear localization of fSAM and bSAM, we generated expression vectors for the NLS-deleted forms of human, feline and bovine SAMHD1 (hSAM△NLS, fSAM△NLS and bSAM△NLS) with HA tags, then fused EGFP to N-terminus of the WT or NLS-deleted SAMHD1 proteins, and tested the different constructs for expression and SAMHD1 intracellular distribution in HEK293 cells. The expression of EGFP-fused SAMHD1 proteins in the transfected HEK293 cells was first analyzed by Western blotting (Fig. 1B). Next, the intracellular distribution of these SAMHD1 proteins in HEK293 cells was analyzed by immunofluorescence experiments. Compared to the intracellular distribution of EGFP expressed by a control vector pVR1012-EGFP in both the nucleus and cytoplasm, all WT SAMHD1 proteins were localized to the nucleus of HEK293 cells (Fig. 1C). By contrast, all SAMHD1 variants missing the NLS were localized to the cytoplasm, indicating that the ^{11}KRPR^{14} sequence also acts as the nuclear localization signal of fSAM and bSAM. Further quantification of the percentage of nuclear SAMHD1 in the WT and NLS-deleted SAMHD1-expressing cells demonstrated that averagely 94.8% and 15.2% of hSAM and hSAM△NLS, 90.6% and 30.6% of fSAM and fSAM△NLS, and 92.2% and 18.1% of bSAM and bSAM△NLS were localized to the nucleus across the cell population, respectively (Fig. 1D). The percentage of fSAM△NLS in the nucleus was significantly higher than that of hSAM△NLS. We also investigated the relative abundance of SAMHD1 protein in nuclear and cytoplasmic extracts by Western blotting (Fig. 1E). After normalized by the level of histone H3 in the nuclear extracts, the relative level of fSAM△NLS detected in the nucleus of HEK293 cells was averagely 34.6% of its WT SAMHD1 protein in the nucleus, which was significantly higher than those percentages of hSAM△NLS and bSAM△NLS (17.8% and 20.8%, respectively, Fig. 1F). However, the percentages of all WT SAMHD1 proteins distributed in the cytoplasm relative to their NLS-deleted variants in the cytoplasm were similar (in a range from 16.0% to 20.6%). These results suggested that feline SAMHD1 may have an additional nucleus-targeting mechanism in addition to the classical NLS.

Cytoplasmic Feline and Bovine SAMHD1 Retain Antiviral Activity against Different Lentiviruses

Both nuclear and cytoplasmic forms of human SAMHD1 could restrict HIV-1 efficiently in stably-transfected U937 and SAMHD1-silenced THP-1 cell lines (Brandariz-Nunez *et al.* 2012). To understand how intracellular distribution influences the antiviral abilities of feline and bovine SAMHD1 and whether they have differences in restriction of different lentiviruses, we first utilized a previously-established quick detection method by using TZM-bl cells (Wang *et al.* 2020). The cells were transfected with WT or NLS-deleted human, feline or bovine SAMHD1 expression vector or empty vector and were then infected with HIV-1, SIVmac239 or HIV-2 ROD at 48 h post-transfection. 48 h later, the infected cells were stained with the substrate of β-galactosidase (X-Gal) and the viral infectivity was determined by the number of positive blue cells. The results showed that hSAM△NLS, fSAM△NLS and bSAM△NLS restricted HIV-1 as efficiently as their WT SAMHD1 proteins (Fig. 2A). hSAM△NLS and fSAM△NLS demonstrated significantly enhanced antiviral activities in restriction of SIVmac239 and HIV-2 ROD compared to their WT SAMHD1 proteins (Fig. 2B, 2C). However, bSAM and bSAM△NLS restricted SIVmac239 and HIV-2 ROD similarly. We also investigated how these SAMHD1 proteins restricted FIV. Because infection of the FIV-GFP pseudovirus cannot generate the blue staining reaction in TZM-bl cells, we infected HEK293T cells with this virus, which had already been transfected with the same SAMHD1-expressing plasmids, and detected the percentage of GFP-positive cells by flow cytometry at 48 h post-infection. No difference was found in the antiviral activity of each of the three pairs of WT and NLS-deleted SAMHD1 proteins against FIV-GFP (Fig. 2D and Supplementary Fig. S1). At the same time, we confirmed that the intracellular levels of the three pairs of WT and NLS-deleted SAMHD1 proteins in the transfected TZM-bl and HEK293T cells were equal before infection, to exclude the possibility of dose-related fluctuation of antiviral activity resulting from different protein expression levels (Supplementary Fig. S2A and S2B).

To further validate these results, we detected the dynamic changes of viral replication of HIV-1, SIVmac239 and HIV-2 ROD and the viral restriction effect after infection with increasing amounts of FIV-GFP in stable U937 cell lines expressing the WT or NLS-deleted SAMHD1 proteins. The results showed that all of the SAMHD1 NLS variants restricted HIV-1 and FIV-GFP as efficiently as their WT proteins (Fig. 3A, 3D). Consistent

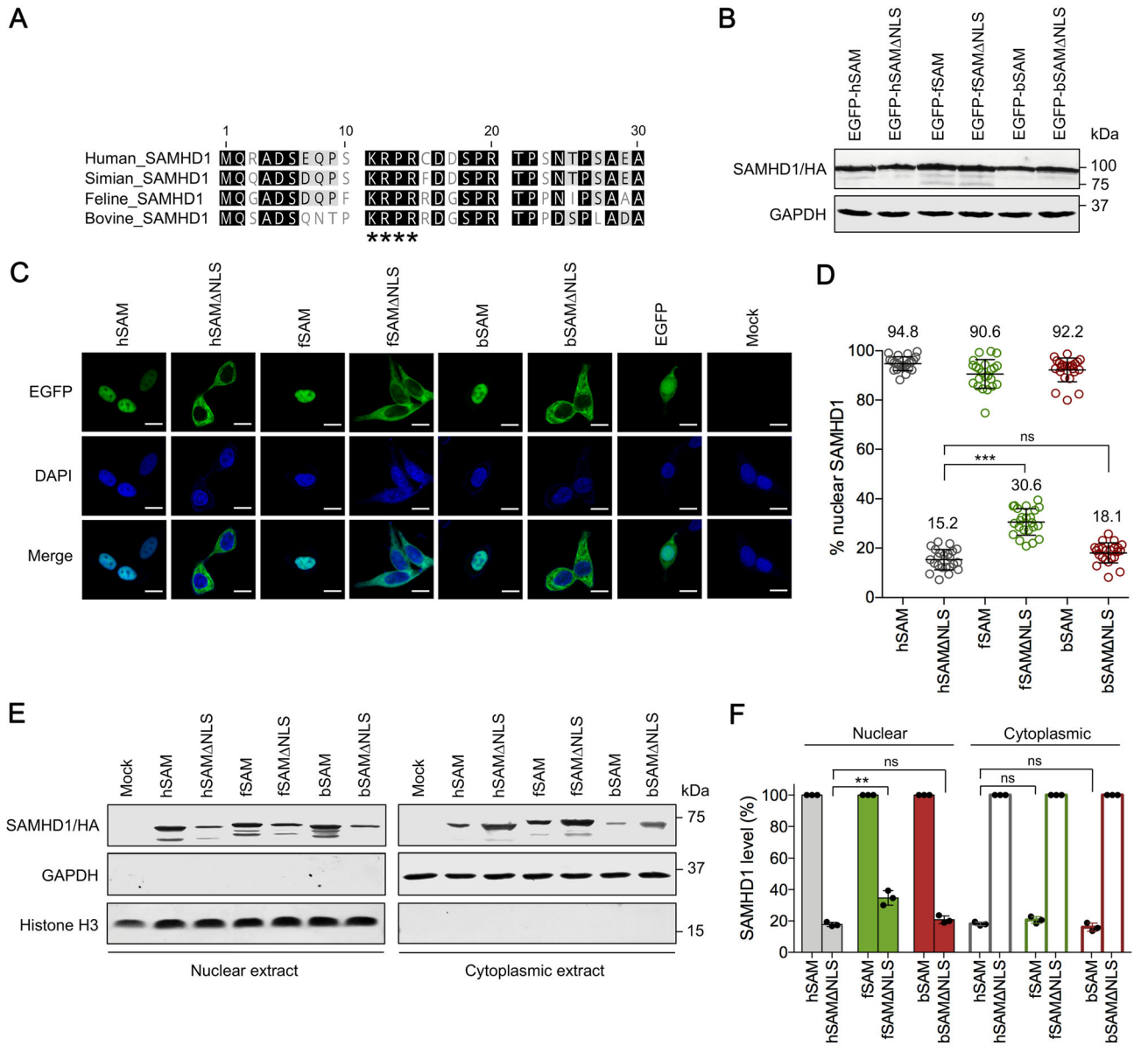

Fig. 1 Identification of ^{11}KRPR^{14} as the functional nuclear localization signal (NLS) of feline and bovine SAMHD1. **A** Alignment of the first 30 amino acids of human, simian, feline and bovine SAMHD1 proteins. The ^{11}KRPR^{14} residue is indicated by asterisks. **B** Expression of enhanced green fluorescent protein (EGFP)-fused wild-type (WT) and NLS-deleted SAMHD1 proteins in HEK293 cells. 48 h post-transfection, the cell lysates of HEK293 cells were analyzed by Western blotting using anti-hemagglutinin (HA) antibody to detect the indicated SAMHD1 proteins with C-terminal HA-tags. GAPDH was detected as a loading control. **C** Intracellular distribution of WT and NLS-deleted SAMHD1 proteins in HEK293 cells. HEK293 cells expressing the indicated EGFP-fused SAMHD1 proteins (green) were fixed and detected by confocal laser scanning microscopy. Cellular nuclei were stained by DAPI (blue). White scale bars, 10 μm. **D** Quantification of the percentage of nuclear SAMHD1 for EGFP-fused WT and NLS-deleted SAMHD1-expressing cells. Each circle represents one cell and the numbers indicate average percentages of cells shown. Statistical analysis was performed between the indicated groups using unpaired Student's *t*-test. **E** Detection of SAMHD1 by Western blotting in nuclear and cytoplasmic extracts of HEK293 cells. Samples were collected at 48 h post-transfection. Histone H3 and GAPDH were detected as nuclear and cytoplasmic protein loading controls, respectively. **F** Quantitation of the band intensity of nuclear and cytoplasmic SAMHD1 of the Western blotting results in HEK293 cells. SAMHD1 band intensities were quantified using Adobe Photoshop and normalized by the level of histone H3 or GAPDH. The percentage of normalized NLS-deleted SAMHD1 proteins in the nuclear extract or WT SAMHD1 proteins in the cytoplasmic extract was calculated relative to that of the corresponding WT or NLS-deleted SAMHD1 proteins (set to 100%, respectively). Error bars represent the SD calculated from three independent experiments. Statistical analysis was performed between the indicated groups using unpaired Student's *t*-test. **Indicates $P \leq 0.01$; *** indicates $P \leq 0.001$; *ns* indicates no significance.

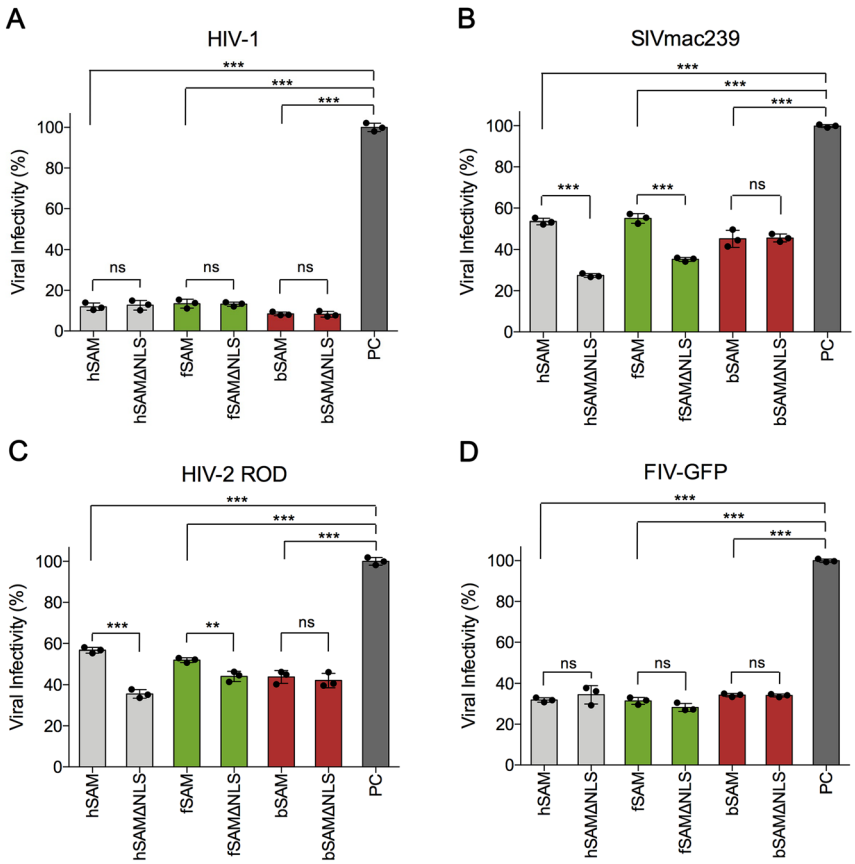

Fig. 2 The antiviral activity of WT and NLS-deleted SAMHD1 proteins against different lentiviruses. **A–C** TZM-bl cells (2×10^6) were transfected with 1.5 μg WT or NLS-deleted human, feline or bovine SAMHD1-HA expression plasmids or empty vector and then infected with (**A**) HIV-1 NL4-3 (0.1 ng of reverse transcriptase, RT), (**B**) SIVmac239 (1 ng of RT) or (**C**) HIV-2 ROD (1 ng of RT) at 48 h post-transfection. Viral infectivity was determined by the number of positive blue cells stained with X-gal. **D** HEK293T cells (2×10^6) were transfected with 400 ng WT or NLS-deleted human, feline or bovine SAMHD1-HA expression plasmids or empty vector and then infected with FIV-GFP (multiplicities of infection, MOI = 0.5) at 48 h post-transfection. Viral infectivity was determined by the percentage of GFP-positive cells quantified by flow cytometry. The viral infectivity in empty vector-transfected cells was set to 100% (positive control, PC). Error bars represent the standard deviation (SD) calculated from three independent infections. Statistical analysis was performed between he indicated groups using unpaired Student's *t*-test. **Indicates $P \leq 0.01$; *** indicates $P \leq 0.001$; *ns* indicates no significance.

with the results obtained in TZM-bl cells, the restriction efficiency of hSAM△NLS and fSAM△NLS against SIVmac239 and HIV-2 ROD was significantly higher than that of their WT proteins, while the restriction efficiency of bSAM and bSAM△NLS against these two viruses was comparable (Fig. 3B, 3C). Immunoblotting analysis of the stable U937 cells showed that the three pairs of WT and NLS-deleted SAMHD1 proteins were expressed at similar levels, respectively (Supplementary Fig. S2C). Together, these results indicated that cytoplasmic feline and bovine SAMHD1 retain the activity to inhibit the infection and replication of different lentiviruses.

Cytoplasmic Bovine SAMHD1 Does Not Resist Vpx-Induced Degradation

It is known that Vpx is encoded by HIV-2 and some strains of SIV to counteract human SAMHD1-mediated restriction by recruiting the $CRL4^{DCAF1}$ E3 ubiquitin ligase complex, leading to the ubiquitination and proteasomal degradation of hSAM (Hrecka *et al.* 2011; Laguette *et al.* 2011; Ahn *et al.* 2012). However, cytoplasmic hSAM is less sensitive to Vpx-induced degradation (Brandariz-Nunez *et al.* 2012; Hofmann *et al.* 2012; Wei *et al.* 2012). Therefore, we hypothesized that the resistance of cytoplasmic SAMHD1 to Vpx-induced degradation leads to the sensitivity of SIV and HIV-2 to cytoplasmic SAMHD1-mediated restriction. Previously, we found that both WT fSAM and bSAM could be proteasomally degraded in the presence of Vpx,

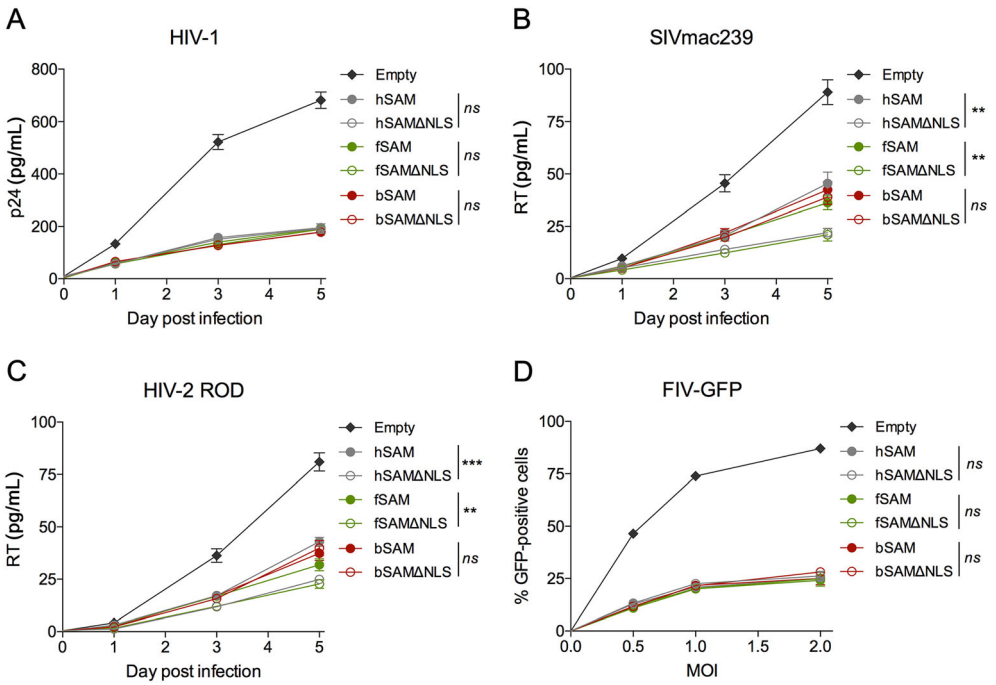

Fig. 3 Restriction of viral infection and replication mediated by WT and NLS-deleted SAMHD1 proteins in U937 cells. **A**–**D** Empty U937 cells (5×10^5) or U937 cells stably expressing WT or NLS-deleted human, feline or bovine SAMHD1 protein were differentiated with PMA for 20 h and infected with (**A**) HIV-1 NL4-3 (0.1 ng of RT), (**B**) SIVmac239 (1 ng of RT), (**C**) HIV-2 ROD (1 ng of RT) or (**D**) FIV-GFP (MOI = 0.5, 1.0 and 2.0). The viral replication curves in (**A**–**C**) were measured by the concentration of p24 for HIV-1 or RT for SIV and HIV-2 in the culture supernatants collected on the day of infection (day 0) and at day 1, 3 and 5 post-infection. The percentage of GFP-positive cells in (**D**) was determined by flow cytometry. Error bars represent the SD calculated from three independent infections. Statistical analysis was performed between groups of each pairs of WT and NLS-deleted SAMHD1 proteins using repeated-measure analysis of two-way ANOVA. **Indicates $P \leq 0.01$; *** indicates $P \leq 0.001$; *ns* indicates no significance.

although they were naturally less sensitive to Vpx-mediated degradation than hSAM (Wang *et al.* 2020). To test whether cytoplasmic fSAM and bSAM is more resistant to Vpx-induced degradation than their WT proteins, Vpx from SIVmac239 and HIV-2 ROD strains (Vpx_{mac} and Vpx_{ROD}) and their Q76A mutants ($Vpx_{mac/Q76A}$ and $Vpx_{ROD/Q76A}$), which no longer bind DCAF1 and were found unable to induce the degradation of SAMHD1 (Srivastava *et al.* 2008; Bergamaschi *et al.* 2009; Hrecka *et al.* 2011), were analyzed for the abilities to counteract WT or NLS-deleted human, feline and bovine SAMHD1 proteins in HEK293 cells. In agreement with previous results (Brandariz-Nunez *et al.* 2012; Hofmann *et al.* 2012), hSAM△NLS was more resistant to both Vpx_{mac} and Vpx_{ROD}-mediated degradation than WT hSAM, and the Vpx_{Q76A} mutants no longer induced the degradation of hSAM and hSAM△NLS (Fig. 4A, 4D, 4G, 4J). fSAM△NLS also showed enhanced resistance to Vpx_{mac} and Vpx_{ROD}-induced degradation than its WT protein (Fig. 4B, 4E, 4H, 4K). However, bSAM and bSAM△NLS were degraded equally in the presence of both Vpx_{mac} and Vpx_{ROD} (Fig. 4C, 4F, 4I, 4L). Although in the presence of $Vpx_{mac/Q76A}$ and $Vpx_{ROD/Q76A}$, the degradation of bSAM△NLS was not recovered, the proteasome inhibitor MG132 treatment suppressed Vpx_{mac} and Vpx_{ROD}-induced degradation of bSAM and bSAM△NLS (Supplementary Fig. S3). Next, we repeated the immunoblotting analysis of fSAM and fSAM△NLS in a feline kidney epithelial cell line, CrFK. Co-expression with Vpx_{mac} or Vpx_{ROD} induced less degradation of fSAM△NLS than that of WT fSAM in this feline cell line (Fig. 5A–5D). We then examined the degradation of fSAM and fSAM△NLS induced by SIVmac239 provirus-expressing plasmids with or without Vpx expression (pSIV or pSIVVpx) in CrFK cells. Results showed that fSAM△NLS was about 30% less sensitive to WT SIVmac239-induced degradation than WT fSAM (Fig. 5E, 5F). We also tried to repeat these detections for bSAM and bSAM△NLS in a cell line of their own species. However, due to the low transfection efficiency of the Madin-Darby bovine kidney (MDBK) cell line we have, we could not obtain a clearly repeated result of the degradation assay of bSAM and bSAM△NLS in this cell line. Still, these results indicated that feline SAMHD1 degradation in response to Vpx requires nuclear localization, while bovine SAMHD1 degradation does not require it.

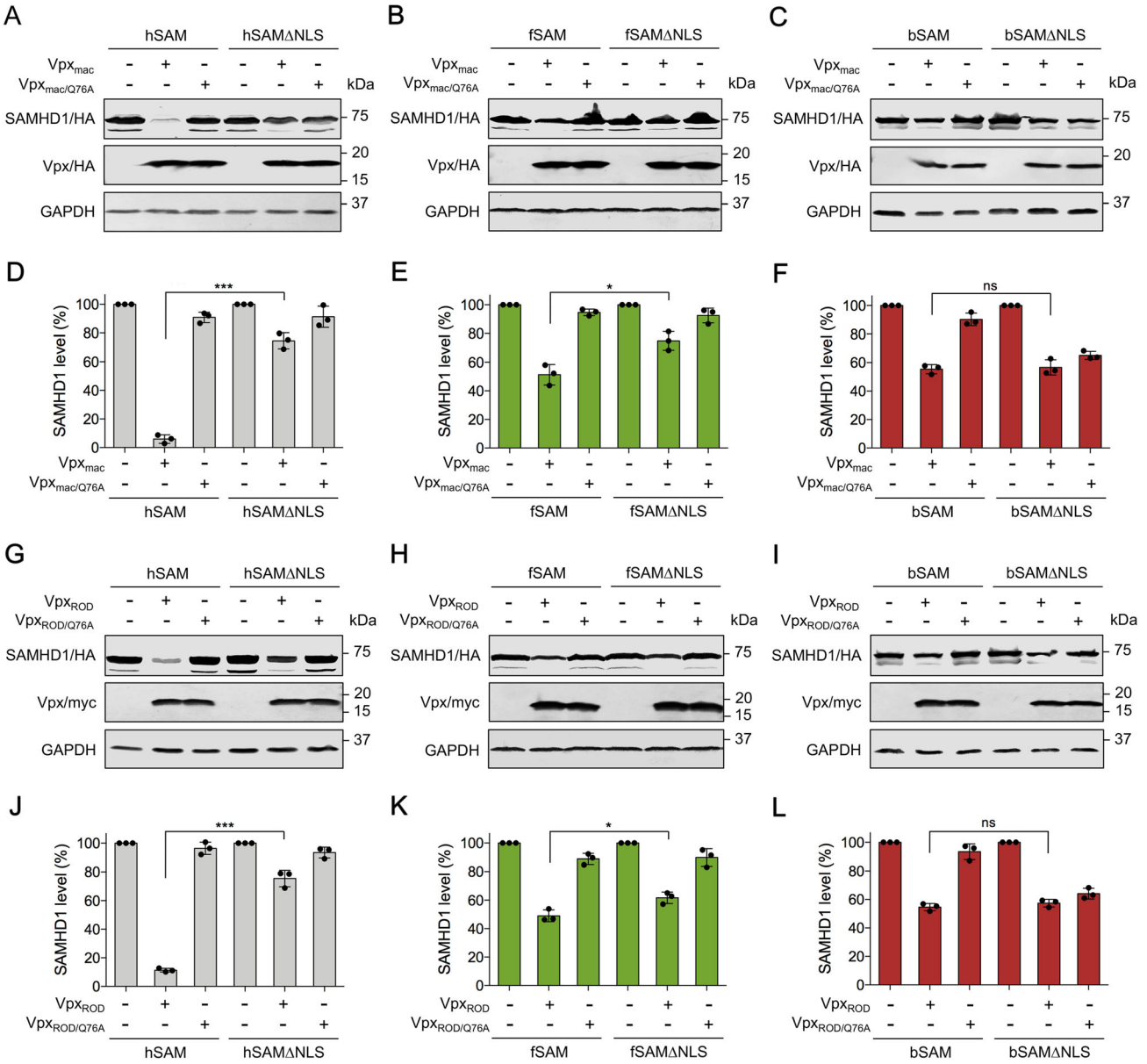

Fig. 4 Cytoplasmic SAMHD1 is partially resistant to Vpx-induced degradation. **A–C** and **G–I** HEK293 cells (1×10^6) were co-transfected with 600 ng of WT or NLS-deleted (**A**, **G**) human (**B**, **H**) feline or (**C**, **I**) bovine SAMHD1-HA expression plasmids and 500 ng of pCG-Vpx_{mac}-HA, pCG-$Vpx_{mac/Q76A}$-HA, pVR1012-Vpx_{ROD}-myc or pVR1012-$Vpx_{ROD/Q76A}$-myc or empty vector. Cells were harvested at 48 h post-transfection and then analyzed by Western blotting using anti-HA, anti-myc, and anti-GAPDH antibodies. **D–F** and **J–L** Quantitation of SAMHD1 band intensity of the Western blotting results in HEK293 cells. The GAPDH-normalized percentage of SAMHD1 level in the presence of Vpx_{mac}, Vpx_{ROD} or the Vpx mutants was calculated relative to that of the corresponding empty vector-co-transfected SAMHD1 (set to 100%, respectively). Error bars represent the SD calculated from three independent experiments. Statistical analysis was performed between the indicated groups using unpaired Student's *t*-test. * indicates $P \leq 0.05$; *** Indicates $P \leq 0.001$; *ns* indicates no significance.

Both Nuclear and Cytoplasmic Feline and Bovine SAMHD1 Have Equal dNTPase Activity and Vpx Binding Capacity

Next, we investigated whether the phenomenon that human and feline cytoplasmic SAMHD1 are less sensitive to Vpx-induced degradation still exist when Vpx is expressed by lentivirus rather than by plasmid transfection. HEK293 cells were first infected with Lenti-Vpx_{ROD} pseudoviruses carrying the *vpx* gene of HIV-2 ROD for 24 h, then transfected with WT or NLS-deleted human, feline and bovine SAMHD1-expressing plasmids. 48 h later, the intracellular level of SAMHD1 was determined by Western blotting. The remaining percentage of WT human, feline

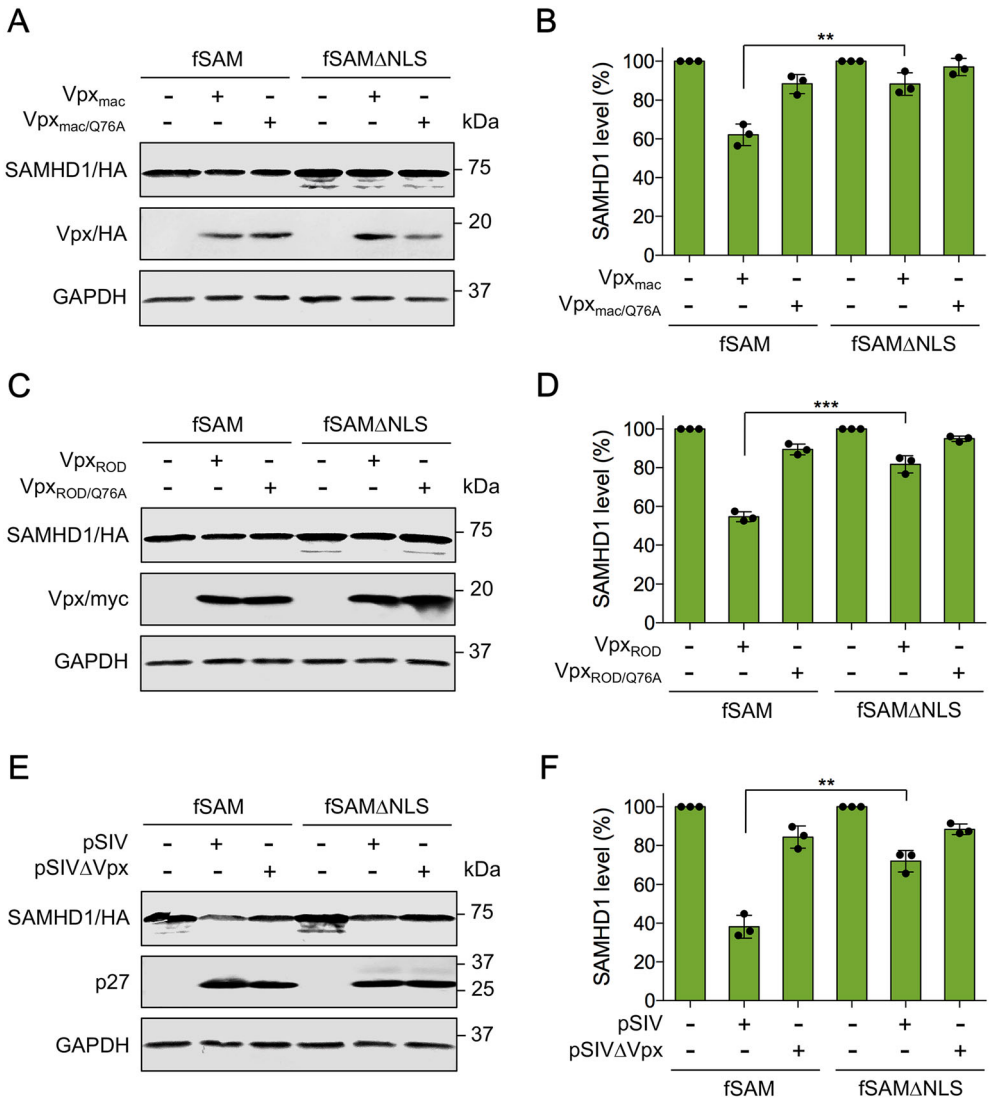

Fig. 5 Vpx-induced degradation of WT and NLS-deleted feline SAMHD1 in CrFK cells. **A**, **C**, **E** CrFK cells (1×10^6) were co-transfected with 600 ng of WT or NLS-deleted feline SAMHD1-HA expression plasmids and 500 ng of (**A**) pCG-Vpx_{mac}-HA or pVR1012-$Vpx_{mac/Q76A}$-HA, (**C**) pCG-Vpx_{ROD}-myc or pVR1012-$Vpx_{ROD/Q76A}$-myc, or 1 μg of (**E**) pSIVmac239 or pSIVmac239ΔVpx, or empty vector. Cells were harvested at 48 h post-transfection and then analyzed by Western blotting using anti-HA, anti-myc, anti-p27 and anti-GAPDH antibodies. **B**, **D**, **F** Quantitation of SAMHD1 band intensity of the Western blotting results in HEK293 cells. The GAPDH-normalized percentage of SAMHD1 level in the presence of Vpx_{mac}, Vpx_{ROD} or SIVmac239 was calculated relative to that of the corresponding empty vector-co-transfected SAMHD1 (set to 100%, respectively). Error bars represent the SD calculated from three independent experiments. **Indicates $P \leq 0.01$; ***indicates $P \leq 0.001$.

and bovine SAMHD1 after degradation were about 8.7%, 52.8% and 59.3%, respectively (Fig. 6A). The corresponding percentage of human and feline NLS-deleted mutants in the presence of Vpx_{ROD}-carrying viruses were recovered to 40.4% and 76.1%, respectively, but the percentage of bSAM△NLS was almost not recovered (61.5%). These results indicated that the less sensitivity of hSAM△NLS and fSAM△NLS to Vpx-induced degradation than their nucleus-localized WT proteins may lead to their better viral restriction outcomes.

To determine whether the enhanced antiviral activity of hSAM△NLS and fSAM△NLS was caused by the change of the dNTPase activity due to NLS deletion, we then tested the dNTPase activity of hSAM, fSAM, bSAM and their NLS variants *in vitro*. Catalytically-inactive mutants $hSAM_{H233A}$, $fSAM_{H233A}$ and $bSAM_{H221A}$ were also tested as the negative controls (Wang *et al.* 2020). The SAMHD1 proteins were immunoprecipitated with anti-HA antibody-conjugated agarose beads from transfected HEK293 cells and added to the reaction mixtures containing dGTP as the

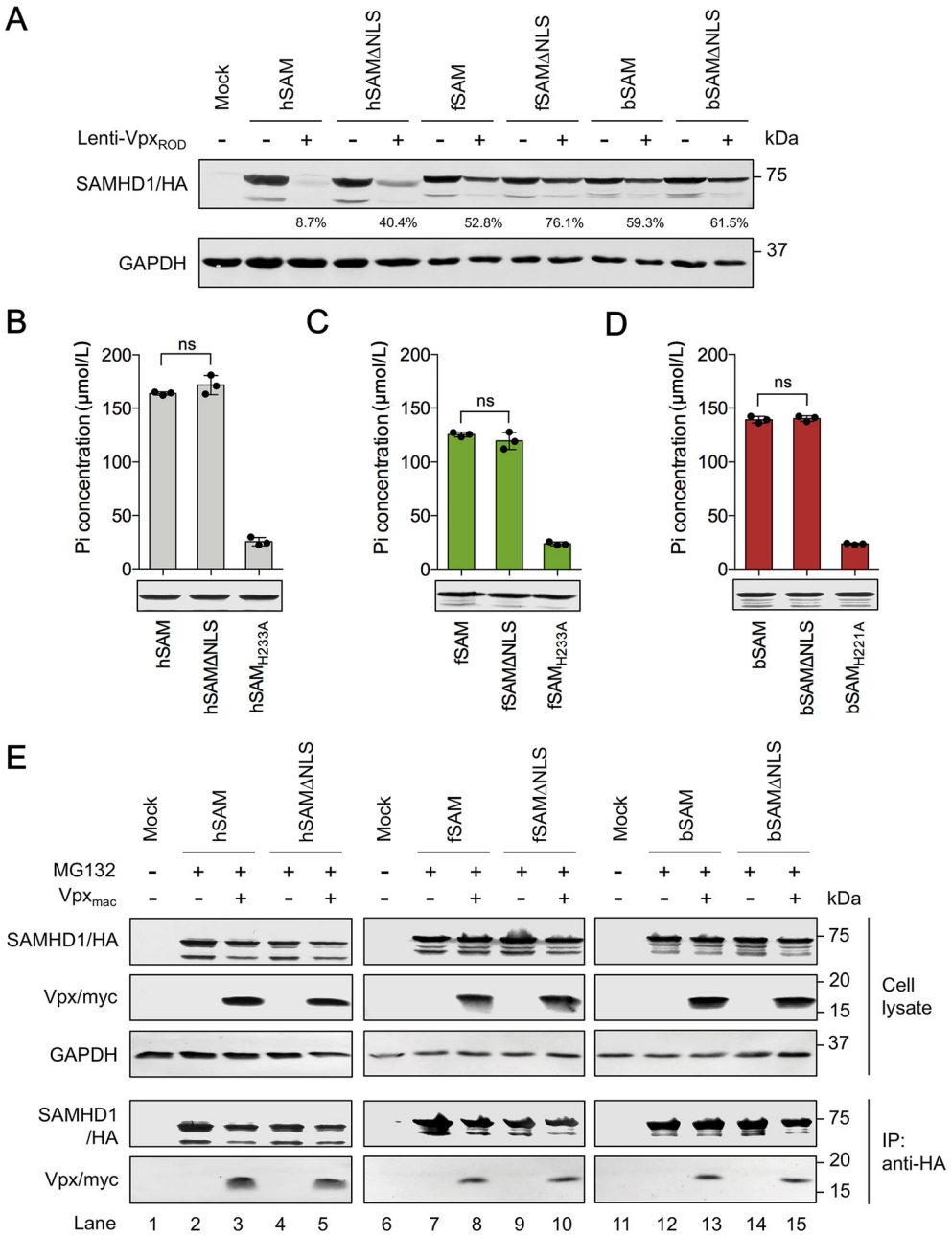

Fig. 6 *In vitro* dNTPase activity comparison and Vpx binding capacity of WT and NLS-deleted SAMHD1 proteins. **A** SAMHD1 degradation mediated by Vpx-expressing lentiviruses. HEK293 cells (5×10^5) were first infected with 3 μg p24 of Lenti-Vpx$_{ROD}$ pseudovirus or incubated with DMEM supplemented with 10% FBS for 24 h, then transfected with 600 ng of WT or NLS-deleted human, feline or bovine SAMHD1-HA expression plasmids or empty vector. Cells were harvested at 48 h post-transfection and then analyzed by Western blotting using anti-HA and anti-GAPDH antibodies. The percentage of SAMHD1 in the presence of Lenti-Vpx$_{ROD}$ was calculated relative to that of the corresponding SAMHD1 in the absence of Lenti-Vpx$_{ROD}$ (set to 100%, respectively). **B**–**D** *In vitro* detection of SAMHD1-catalyzed inorganic phosphate (Pi) release. HA-tagged SAMHD1 proteins were isolated from transfected HEK293 cells by immunoprecipitation. An aliquot of the immunoprecipitated SAMHD1 proteins was analyzed by Western blotting to ascertain comparable protein levels using anti-HA antibody. The levels of Pi released after *in vitro* dGTP-pyrophosphatase hydrolysis reactions were detected by malachite green. Error bars represent the SD calculated from three independent reactions. Statistical analysis was performed between the indicated groups using unpaired Student's *t*-test. **E** Detection of the interaction between Vpx and SAMHD1 by co-immunoprecipitation. HEK293 cells (2×10^6) were co-transfected with WT or NLS-deleted human, feline or bovine SAMHD1-HA expression plasmids and 1.0 μg pVR1012-Vpx$_{mac}$-myc or empty vector. All transfected cells were incubated with the proteasome inhibitor MG132 at 20 μmol/L for 12 h before harvesting. 48 h post-transfection, cell lysates were immunoprecipitated with anti-HA antibody-conjugated beads, followed by Western blotting with anti-HA, anti-myc and anti-GAPDH antibodies. *ns* indicates no significance.

substrate and pyrophosphatase to hydrolyze the triphosphate product of SAMHD1. The final product inorganic phosphate (Pi) of hydrolysis was quantified by malachite green to determine the dNTPase activity. The results demonstrated that NLS deletion did not impact the dNTPase activity of all SAMHD1 proteins from the three species (Fig. 6B–6D).

Previous studies showed that Vpx_{mac} and Vpx_{ROD} can interact with both nuclear and cytoplasmic forms of human SAMHD1 (Hofmann *et al.* 2012; Schaller *et al.* 2014). To understand the different sensitivity of cytoplasmic fSAM and bSAM to Vpx-mediated degradation, we investigated whether cytoplasmic feline and bovine SAMHD1 still interact with Vpx. The interactions between SIVmac239 Vpx and hSAM, fSAM or bSAM or their variants with NLS deletion were analyzed by co-immunoprecipitation experiments. Myc-tagged Vpx_{mac} and HA-tagged WT SAMHD1 or the NLS variants were co-expressed in HEK293 cells and the transfected cells were treated with MG132 for 12 h before harvest. The cell lysates were subjected to co-immunoprecipitation using anti-HA beads at 48 h post-transfection. The anti-HA beads immunoprecipitated WT SAMHD1 as well as the NLS variants from cell lysates of the transfected HEK293 cells (Fig. 6E). We observed co-precipitation of myc-tagged Vpx with all WT or NLS-deleted human, feline and bovine SAMHD1 proteins (lanes 3, 5, 8, 10, 13 and 15), indicating that all of the three cytoplasmic SAMHD1 proteins have similar Vpx binding capacity to the corresponding WT SAMHD1 proteins. Taken together with previous results, these data suggested that feline cytoplasmic SAMHD1 can suppress more SIV and HIV-2 infection and replication than its WT protein by being less sensitive to Vpx-mediated degradation as human cytoplasmic SAMHD1 rather than having higher dNTPase activity and that the less degradation of cytoplasmic human and feline SAMHD1 than their nucleus-localized WT proteins in the presence of Vpx is not caused by different Vpx binding capacity.

Discussion

To gain more knowledge of SAMHD1 from different species can provide a deeper understanding of this host-derived viral restriction factor from an evolutionary view and facilitate the establishment of animal models to understand the physiological role of SAMHD1 *in vivo*. SAMHD1 proteins of monkeys (Fregoso *et al.* 2013; Wei *et al.* 2014; Li *et al.* 2015; Schwefel *et al.* 2015; Shingai *et al.* 2015; Buchanan *et al.* 2016) and mice (Behrendt *et al.* 2013; Zhang *et al.* 2014; Wang *et al.* 2016; Bloch *et al.* 2017; Buzovetsky *et al.* 2018) have been intensively investigated for their roles in lentiviral restriction as well as for their structure, dNTPase activity and roles in the regulation of the innate immune responses. The characteristics of feline and bovine SAMHD1 have also been studied by several groups and us (Asadian *et al.* 2018; Mereby *et al.* 2018; Asadian and Bienzle 2019; Wang *et al.* 2020). However, the non-primate animal model of SAMHD1 has only been established in mice and knowledge of other non-primate SAMHD1 proteins is limited. To find out more information of common and different features between the primate and non-primate SAMHD1 proteins will contribute to the improvement of SAMHD1-knockout small animal models.

A previous study of human SAMHD1 showed its distribution in both the nucleus and cytoplasm of resting $CD4^+$ T cells, activated $CD4^+$ T cells, and macrophages in immunoblots of nuclear and cytoplasmic fractions and 3D-reconstructed confocal images (Baldauf *et al.* 2012), but it is mainly localized to the nucleus when observed by confocal microscopy in Hela and U937 cells (Brandariz-Nunez *et al.* 2012; Hofmann *et al.* 2012). Study of the expression profile of SAMHD1 in feline tissues by immunohistochemical staining demonstrated that although feline SAMHD1 is predominantly localized to the nucleus, the expression level of SAMHD1 in the nucleus relative to that in the cytoplasm was variable in different tissues (Asadian *et al.* 2018). These results suggest that SAMHD1 is positioned into the nucleus after protein synthesis in the cytoplasm and detection of cytoplasmic SAMHD1 may reflect recently translated protein, and additionally, that SAMHD1 may be regulated by certain signals such as cytokines or phosphorylation to balance its nuclear/cytoplasmic distribution ratio in different cell lines. This can be supported by a recent study in which interferon-γ treatment was found being able to increase SAMHD1 translocation to the nucleus in primary feline $CD4^+$ T lymphocytes (Asadian and Bienzle 2019). In the current study, we first investigated whether the NLS sequence ^{11}KRPR^{14} identified in human SAMHD1 is also the key NLS in feline and bovine SAMHD1. Our quantification results of the nucleus-localized WT and NLS-deleted SAMHD1 proteins in the whole SAMHD1-expressing cells (Fig. 1D) and the immunoblotting result of the SAMHD1 proteins in nuclear and cytoplasmic fractions (Fig. 1E, 1F) demonstrated that feline NLS-deleted SAMHD1 had the highest occupation rate in the nucleus among the three NLS-deleted SAMHD1 proteins, suggesting that in addition to the N-terminal ^{11}KRPR^{14} which acts as the major signal for nuclear import, feline SAMHD1 may have other signals to maintain it inside the nucleus. Some residues in feline SAMHD1 may also contribute to its nuclear localization, which is supported by the findings that mutations such as I201N, R226G and M254V of human SAMHD1 found in AGS

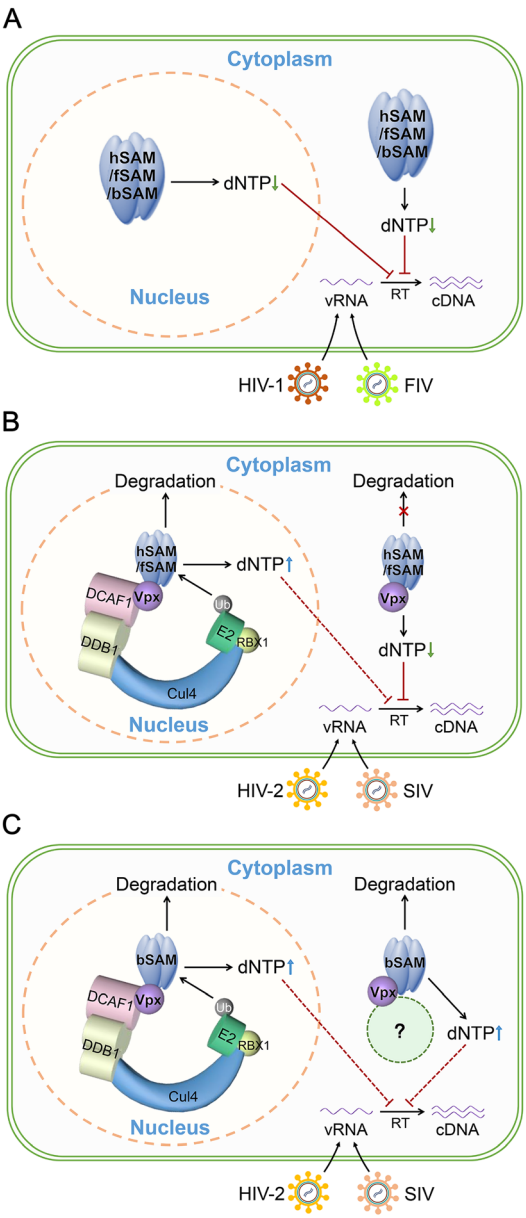

Fig. 7 Proposed mechanism of feline and bovine SAMHD1-mediated lentiviral restriction and Vpx-mediated counteraction on different SAMHD1 proteins. **A** Each of tetrameric hSAM, fSAM and bSAM has dNTPase activity and both of the nucleus- and cytoplasm-localized hSAM, fSAM and bSAM can restrict HIV-1 and FIV infection at the RT step by depleting intracellular dNTPs to a low concentration that is insufficient for cDNA synthesis from viral RNA (vRNA). **B** HIV-2 ROD and SIVmac239 Vpx induces degradation of nuclear hSAM or fSAM by targeting it to the $CRL4^{DCAF1}$ E3 ubiquitin ligase complex and adding of ubiquitin (Ub), leading to the increase of intracellular dNTP levels and efficient viral cDNA synthesis. The red dashed line indicates the impaired viral restriction function. While cytoplasmic hSAM and fSAM are resistant to Vpx-induced degradation because Vpx cannot recruit the nucleus-localized $CRL4^{DCAF1}$ E3 ubiquitin ligase complex in the cytoplasm, thus they retain the full antiviral ability. **C** Both nucleus- and cytoplasm-localized bSAM can be degraded in the presence of HIV-2 ROD and SIVmac239 Vpx and their antiviral effects are also similarly impaired, thus an unknown E3 ubiquitin ligase complex (shown as the green dashed circle) which can be recruited by Vpx for specific degradation of bSAM in the cytoplasm may exist.

patients were shown related to partial cytoplasmic accumulation (Goncalves *et al.* 2012; White *et al.* 2017).

Our previous study showed that feline and bovine SAMHD1 could restrict HIV-1, SIV and HIV-2 as efficiently as human SAMHD1 by using their dNTPase activities (Wang *et al.* 2020). Consistent with the results found in human SAMHD1 that SIVmac is not capable of overcoming the restriction imposed by the SAMHD1 NLS mutant (Brandariz-Nunez *et al.* 2012), hSAM△NLS restricted more SIVmac239 and HIV-2 ROD than its WT protein in both TZM-bl and U937 cell lines (Figs. 2, 3). In our experiments, SAMHD1 was over-expressed in these two cell lines before infection and the amounts of quantified viruses used for infection were relatively low, thus, the degradation of SAMHD1 after SIV and HIV-2 infection should be incomplete. However, the difference in the antiviral activity of nuclear and cytoplasmic SAMHD1 could still be significantly seen. fSAM△NLS showed a similar increased antiviral activity than its WT protein against SIVmac239 and HIV-2 ROD as hSAM△NLS, suggesting that Vpx of SIVmac239 and HIV-2 ROD requires nucleus-localized human and feline SAMHD1 to induce their degradation and to overcome restriction (Fig. 7B). While bovine SAMHD1 could be degraded in both the nucleus and cytoplasm, thus the antiviral activity of bovine SAMHD1 was impaired no matter it was localized to the nucleus or the cytoplasm in the presence of Vpx (Fig. 7C). A previous study has reported that FIV and BIV infections do not induce the degradation of their host SAMHD1 proteins (Mereby *et al.* 2018). Therefore, all of the three pairs of nucleus- and cytoplasm-localized SAMHD1 proteins retained complete antiviral activity against HIV-1 and FIV (Fig. 7A). Considering that NLS deletion did not alter the dNTPase activity of SAMHD1 from all of the three species (Fig. 6B–6D), the better antiviral outcome was realized by the higher intracellular level of SAMHD1, confirming that SAMHD1 can deplete the overall cellular pool of dNTPs no matter in the nucleus or the cytoplasm (Brandariz-Nunez *et al.* 2012; Hofmann *et al.* 2012).

Previous studies suggested that Vpx-mediated degradation of human SAMHD1 is initiated in the nucleus (Brandariz-Nunez *et al.* 2012) and found that cytoplasmic human SAMHD1 could interact with Vpx which also has a nuclear localization signal (Pancio *et al.* 2000; Belshan and Ratner 2003) and retained it in the cytoplasm without being degraded (Hofmann *et al.* 2012). By contrast, the level of

nucleus-localized human SAMHD1 is largely determined by Vpx-mediated degradation. Vpx directly binds to human SAMHD1 and simultaneously to the DCAF1 substrate receptor of the CRL4 E3 ubiquitin ligase (Hrecka *et al.* 2011; Ahn *et al.* 2012). DCAF1 was found localized in the nucleus and functioning in this compartment like other CRL4 ligases (Lee and Zhou 2007; Li *et al.* 2010; Guo *et al.* 2019). The cytoplasm-localized DCAF1 truncation mutant inhibits Vpx-mediated degradation of human SAMHD1 (Guo *et al.* 2019). Thus, it could be speculated that the degradation of human SAMHD1 should be confined to the nucleus. Like human SAMHD1, feline SAMHD1 with NLS deletion was less sensitive to Vpx-mediated degradation than its WT protein (Figs. 4, 5), except that the recovery percentage of WT feline SAMHD1 in the presence of Vpx_{Q76A} mutants instead of WT Vpx was lower than that observed in human SAMHD1. There are two possible reasons which can be found from our results for the lower recovery percentage: (1) WT fSAM was less sensitive to Vpx-mediated degradation than WT hSAM, as found in our previous results (Wang *et al.* 2020); (2) NLS-deleted fSAM was not totally localized to the cytoplasm as shown in Fig. 1. Surprisingly, we found that bovine SAMHD1 was sensitive to Vpx-induced proteasomal degradation in both the nucleus and cytoplasm (Supplementary Fig. S3), but in the presence of the Q76A mutants of both SIVmac239 and HIV-2 ROD Vpx which is essential in Vpx-DCAF1 binding, the degradation of bSAM△NLS was not recovered significantly as what was observed in hSAM△NLS and fSAM△NLS (Fig. 4). We further showed that both nucleus- and cytoplasm-localized bovine SAMHD1 proteins have similar Vpx binding capacity as human and feline SAMHD1 (Fig. 6C). Therefore, these results suggested that bovine SAMHD1 may not be degraded only through the $CRL4^{DCAF1}$ E3 ubiquitin ligase complex, which is different from human and feline SAMHD1 (Fig. 7). Vpx may recruit another E3 ubiquitin ligase complex for degradation of cytoplasmic bovine SAMHD1 (Fig. 7C). Further investigation is needed to find out why only bovine SAMHD1 rather than human or feline SAMHD1 can become the substrate of this complex in the cytoplasm.

Taken together, our study supported that the lentiviral Vpx protein primarily targets nucleus-localized SAMHD1 by utilizing the E3 ubiquitin ligase complex which is also localized to the nucleus but may also have additional degradation mechanisms when countering sequence-divergent SAMHD1 proteins and suggested that feline SAMHD1 shares more common features with human SAMHD1, thus is more suitable for the establishment of the animal model to study SAMHD1 *in vivo*.

Acknowledgements This research was funded by the National Natural Science Foundation of China (31270807), the Key Projects in the National Science & Technology Pillar Program in the Thirteenth Five-year Plan Period (2018ZX10731101-002-003 and 2018ZX10731101-001-020), Program for Jilin University Science and Technology Innovative Research Team (JLUSTIRT) (2017TD-05), National Postdoctoral Program for Innovative Talents (BX20180124), China Postdoctoral Science Foundation (2018M641786), and Science and Technology Development Project of Jilin Province (20200901030SF).

Author contributions CW, JXW and XHY designed the experiments. CW, LNM, JLW, KKZ, SZD, PYR, YZW and XYF carried out the experiments. CW and LNM analyzed the data and wrote the paper. BY, JXW and XHY checked and finalized the manuscript. CW and XHY acquired the funding. All authors read and approved the final manuscript.

Compliance with Ethical Standards

Conflict of interest The authors declare that they have no conflict of interest.

Animal and Human Rights Statement This article does not contain any studies with human or animal subjects performed by any of the authors.

References

Ahn J, Hao C, Yan J, DeLucia M, Mehrens J, Wang C, Gronenborn AM, Skowronski J (2012) HIV/simian immunodeficiency virus (SIV) accessory virulence factor Vpx loads the host cell restriction factor SAMHD1 onto the E3 ubiquitin ligase complex CRL4DCAF1. J Biol Chem 287:12550–12558

Amie SM, Bambara RA, Kim B (2013) GTP is the primary activator of the anti-HIV restriction factor SAMHD1. J Biol Chem 288:25001–25006

Asadian P, Bienzle D (2019) Interferon gamma and alpha have differential effects on SAMHD1, a potent antiviral protein, in feline lymphocytes. Viruses 11:921

Asadian P, Finnie G, Bienzle D (2018) The expression profile of sterile alpha motif and histidine-aspartate domain-containing protein 1 (SAMHD1) in feline tissues. Vet Immunol Immunopathol 195:7–18

Baldauf HM, Pan X, Erikson E, Schmidt S, Daddacha W, Burggraf M, Schenkova K, Ambiel I, Wabnitz G, Gramberg T, Panitz S, Flory E, Landau NR, Sertel S, Rutsch F, Lasitschka F, Kim B, Konig R, Fackler OT, Keppler OT (2012) SAMHD1 restricts HIV-1 infection in resting CD4(+) T cells. Nat Med 18:1682–1687

Behrendt R, Schumann T, Gerbaulet A, Nguyen LA, Schubert N, Alexopoulou D, Berka U, Lienenklaus S, Peschke K, Gibbert K, Wittmann S, Lindemann D, Weiss S, Dahl A, Naumann R, Dittmer U, Kim B, Mueller W, Gramberg T, Roers A (2013) Mouse SAMHD1 has antiretroviral activity and suppresses a spontaneous cell-intrinsic antiviral response. Cell Rep 4:689–696

Belshan M, Ratner L (2003) Identification of the nuclear localization signal of human immunodeficiency virus type 2 Vpx. Virology 311:7–15

Bergamaschi A, Ayinde D, David A, Le Rouzic E, Morel M, Collin G, Descamps D, Damond F, Brun-Vezinet F, Nisole S,

Margottin-Goguet F, Pancino G, Transy C (2009) The human immunodeficiency virus type 2 Vpx protein usurps the CUL4A-DDB1 DCAF1 ubiquitin ligase to overcome a postentry block in macrophage infection. J Virol 83:4854–4860

Berger G, Turpin J, Cordeil S, Tartour K, Nguyen XN, Mahieux R, Cimarelli A (2012) Functional analysis of the relationship between Vpx and the restriction factor SAMHD1. J Biol Chem 287:41210–41217

Bhattacharya A, Wang Z, White T, Buffone C, Nguyen LA, Shepard CN, Kim B, Demeler B, Diaz-Griffero F, Ivanov DN (2016) Effects of T592 phosphomimetic mutations on tetramer stability and dNTPase activity of SAMHD1 can not explain the retroviral restriction defect. Sci Rep 6:31353

Bloch N, Glasker S, Sitaram P, Hofmann H, Shepard CN, Schultz ML, Kim B, Landau NR (2017) A highly active isoform of lentivirus restriction factor SAMHD1 in mouse. J Biol Chem 292:1068–1080

Brandariz-Nunez A, Valle-Casuso JC, White TE, Laguette N, Benkirane M, Brojatsch J, Diaz-Griffero F (2012) Role of SAMHD1 nuclear localization in restriction of HIV-1 and SIVmac. Retrovirology 9:49

Buchanan EL, Espinoza DA, McAlexander MA, Myers SL, Moyer A, Witwer KW (2016) SAMHD1 transcript upregulation during SIV infection of the central nervous system does not associate with reduced viral load. Sci Rep 6:22629

Buzovetsky O, Tang C, Knecht KM, Antonucci JM, Wu L, Ji X, Xiong Y (2018) The SAM domain of mouse SAMHD1 is critical for its activation and regulation. Nat Commun 9:411

Chen Z, Zhu M, Pan X, Zhu Y, Yan H, Jiang T, Shen Y, Dong X, Zheng N, Lu J, Ying S, Shen Y (2014) Inhibition of Hepatitis B virus replication by SAMHD1. Biochem Biophys Res Commun 450:1462–1468

Cribier A, Descours B, Valadao AL, Laguette N, Benkirane M (2013) Phosphorylation of SAMHD1 by cyclin A2/CDK1 regulates its restriction activity toward HIV-1. Cell Rep 3:1036–1043

Descours B, Cribier A, Chable-Bessia C, Ayinde D, Rice G, Crow Y, Yatim A, Schwartz O, Laguette N, Benkirane M (2012) SAMHD1 restricts HIV-1 reverse transcription in quiescent CD4(+) T-cells. Retrovirology 9:87

Fregoso OI, Ahn J, Wang C, Mehrens J, Skowronski J, Emerman M (2013) Evolutionary toggling of Vpx/Vpr specificity results in divergent recognition of the restriction factor SAMHD1. PLoS Pathog 9:e1003496

Goldstone DC, Ennis-Adeniran V, Hedden JJ, Groom HC, Rice GI, Christodoulou E, Walker PA, Kelly G, Haire LF, Yap MW, de Carvalho LP, Stoye JP, Crow YJ, Taylor IA, Webb M (2011) HIV-1 restriction factor SAMHD1 is a deoxynucleoside triphosphate triphosphohydrolase. Nature 480:379–382

Goncalves A, Karayel E, Rice GI, Bennett KL, Crow YJ, Superti-Furga G, Burckstummer T (2012) SAMHD1 is a nucleic-acid binding protein that is mislocalized due to aicardi-goutieres syndrome-associated mutations. Hum Mutat 33:1116–1122

Gramberg T, Kahle T, Bloch N, Wittmann S, Mullers E, Daddacha W, Hofmann H, Kim B, Lindemann D, Landau NR (2013) Restriction of diverse retroviruses by SAMHD1. Retrovirology 10:26

Guo H, Zhang N, Shen S, Yu XF, Wei W (2019) Determinants of lentiviral Vpx-CRL4 E3 ligase-mediated SAMHD1 degradation in the substrate adaptor protein DCAF1. Biochem Biophys Res Commun 513:933–939

Hofmann H, Logue EC, Bloch N, Daddacha W, Polsky SB, Schultz ML, Kim B, Landau NR (2012) The Vpx lentiviral accessory protein targets SAMHD1 for degradation in the nucleus. J Virol 86:12552–12560

Hollenbaugh JA, Gee P, Baker J, Daly MB, Amie SM, Tate J, Kasai N, Kanemura Y, Kim DH, Ward BM, Koyanagi Y, Kim B (2013) Host factor SAMHD1 restricts DNA viruses in non-dividing myeloid cells. PLoS Pathog 9:e1003481

Hrecka K, Hao C, Gierszewska M, Swanson SK, Kesik-Brodacka M, Srivastava S, Florens L, Washburn MP, Skowronski J (2011) Vpx relieves inhibition of HIV-1 infection of macrophages mediated by the SAMHD1 protein. Nature 474:658–661

Ji X, Tang C, Zhao Q, Wang W, Xiong Y (2014) Structural basis of cellular dNTP regulation by SAMHD1. Proc Natl Acad Sci USA 111:E4305–E4314

Ji X, Wu Y, Yan J, Mehrens J, Yang H, DeLucia M, Hao C, Gronenborn AM, Skowronski J, Ahn J, Xiong Y (2013) Mechanism of allosteric activation of SAMHD1 by dGTP. Nat Struct Mol Biol 20:1304–1309

Khare PD, Loewen N, Teo W, Barraza RA, Saenz DT, Johnson DH, Poeschla EM (2008) Durable, safe, multi-gene lentiviral vector expression in feline trabecular meshwork. Mol Ther 16:97–106

Kim B, Nguyen LA, Daddacha W, Hollenbaugh JA (2012) Tight interplay among SAMHD1 protein level, cellular dNTP levels, and HIV-1 proviral DNA synthesis kinetics in human primary monocyte-derived macrophages. J Biol Chem 287:21570–21574

Kim ET, White TE, Brandariz-Nunez A, Diaz-Griffero F, Weitzman MD (2013) SAMHD1 restricts herpes simplex virus 1 in macrophages by limiting DNA replication. J Virol 87:12949–12956

Koharudin LM, Wu Y, DeLucia M, Mehrens J, Gronenborn AM, Ahn J (2014) Structural basis of allosteric activation of sterile alpha motif and histidine-aspartate domain-containing protein 1 (SAMHD1) by nucleoside triphosphates. J Biol Chem 289:32617–32627

Laguette N, Sobhian B, Casartelli N, Ringeard M, Chable-Bessia C, Segeral E, Yatim A, Emiliani S, Schwartz O, Benkirane M (2011) SAMHD1 is the dendritic- and myeloid-cell-specific HIV-1 restriction factor counteracted by Vpx. Nature 474:654–657

Lahouassa H, Daddacha W, Hofmann H, Ayinde D, Logue EC, Dragin L, Bloch N, Maudet C, Bertrand M, Gramberg T, Pancino G, Priet S, Canard B, Laguette N, Benkirane M, Transy C, Landau NR, Kim B, Margottin-Goguet F (2012) SAMHD1 restricts the replication of human immunodeficiency virus type 1 by depleting the intracellular pool of deoxynucleoside triphosphates. Nat Immunol 13:223–228

Lee J, Zhou P (2007) DCAFs, the missing link of the CUL4-DDB1 ubiquitin ligase. Mol Cell 26:775–780

Li J, Xu F, Hu S, Zhou J, Mei S, Zhao X, Cen S, Jin Q, Liang C, Guo F (2015) Characterization of the interactions between SIVrcm Vpx and red-capped mangabey SAMHD1. Biochem J 468:303–313

Li W, You L, Cooper J, Schiavon G, Pepe-Caprio A, Zhou L, Ishii R, Giovannini M, Hanemann CO, Long SB, Erdjument-Bromage H, Zhou P, Tempst P, Giancotti FG (2010) Merlin/NF2 suppresses tumorigenesis by inhibiting the E3 ubiquitin ligase CRL4(DCAF1) in the nucleus. Cell 140:477–490

Li Z, Huan C, Wang H, Liu Y, Liu X, Su X, Yu J, Zhao Z, Yu XF, Zheng B, Zhang W (2020) TRIM21-mediated proteasomal degradation of SAMHD1 regulates its antiviral activity. EMBO Rep 21:e47528

Lim ES, Fregoso OI, McCoy CO, Matsen FA, Malik HS, Emerman M (2012) The ability of primate lentiviruses to degrade the monocyte restriction factor SAMHD1 preceded the birth of the viral accessory protein Vpx. Cell Host Microbe 11:194–204

Mereby SA, Maehigashi T, Holler JM, Kim DH, Schinazi RF, Kim B (2018) Interplay of ancestral non-primate lentiviruses with the virus-restricting SAMHD1 proteins of their hosts. J Biol Chem 293:16402–16412

Pancio HA, Vander Heyden N, Ratner L (2000) The C-terminal proline-rich tail of human immunodeficiency virus type 2 Vpx is

necessary for nuclear localization of the viral preintegration complex in nondividing cells. J Virol 74:6162–6167

Pauls E, Ruiz A, Badia R, Permanyer M, Gubern A, Riveira-Munoz E, Torres-Torronteras J, Alvarez M, Mothe B, Brander C, Crespo M, Menendez-Arias L, Clotet B, Keppler OT, Marti R, Posas F, Ballana E, Este JA (2014) Cell cycle control and HIV-1 susceptibility are linked by CDK6-dependent CDK2 phosphorylation of SAMHD1 in myeloid and lymphoid cells. J Immunol 193:1988–1997

Powell RD, Holland PJ, Hollis T, Perrino FW (2011) Aicardi-Goutieres syndrome gene and HIV-1 restriction factor SAMHD1 is a dGTP-regulated deoxynucleotide triphosphohydrolase. J Biol Chem 286:43596–43600

Rice GI, Bond J, Asipu A, Brunette RL, Manfield IW, Carr IM, Fuller JC, Jackson RM, Lamb T, Briggs TA, Ali M, Gornall H, Couthard LR, Aeby A, Attard-Montalto SP, Bertini E, Bodemer C, Brockmann K, Brueton LA, Corry PC, Desguerre I, Fazzi E, Cazorla AG, Gener B, Hamel BC, Heiberg A, Hunter M, van der Knaap MS, Kumar R, Lagae L, Landrieu PG, Lourenco CM, Marom D, McDermott MF, van der Merwe W, Orcesi S, Prendiville JS, Rasmussen M, Shalev SA, Soler DM, Shinawi M, Spiegel R, Tan TY, Vanderver A, Wakeling EL, Wassmer E, Whittaker E, Lebon P, Stetson DB, Bonthron DT, Crow YJ (2009) Mutations involved in Aicardi-Goutieres syndrome implicate SAMHD1 as regulator of the innate immune response. Nat Genet 41:829–832

Schaller T, Pollpeter D, Apolonia L, Goujon C, Malim MH (2014) Nuclear import of SAMHD1 is mediated by a classical karyopherin alpha/beta1 dependent pathway and confers sensitivity to VpxMAC induced ubiquitination and proteasomal degradation. Retrovirology 11:29

Schwefel D, Boucherit VC, Christodoulou E, Walker PA, Stoye JP, Bishop KN, Taylor IA (2015) Molecular determinants for recognition of divergent SAMHD1 proteins by the lentiviral accessory protein Vpx. Cell Host Microbe 17:489–499

Shingai M, Welbourn S, Brenchley JM, Acharya P, Miyagi E, Plishka RJ, Buckler-White A, Kwong PD, Nishimura Y, Strebel K, Martin MA (2015) The expression of functional Vpx during pathogenic SIVmac Infections of rhesus macaques suppresses SAMHD1 in CD4+ memory T Cells. PLoS Pathog 11:e1004928

Spragg CJ, Emerman M (2013) Antagonism of SAMHD1 is actively maintained in natural infections of simian immunodeficiency virus. Proc Natl Acad Sci USA 110:21136–21141

Srivastava S, Swanson SK, Manel N, Florens L, Washburn MP, Skowronski J (2008) Lentiviral Vpx accessory factor targets VprBP/DCAF1 substrate adaptor for cullin 4 E3 ubiquitin ligase to enable macrophage infection. PLoS Pathog 4:e1000059

St Gelais C, de Silva S, Amie SM, Coleman CM, Hoy H, Hollenbaugh JA, Kim B, Wu L (2012) SAMHD1 restricts HIV-1 infection in dendritic cells (DCs) by dNTP depletion, but its expression in DCs and primary CD4+ T-lymphocytes cannot be upregulated by interferons. Retrovirology 9:105

Tang C, Ji X, Wu L, Xiong Y (2015) Impaired dNTPase activity of SAMHD1 by phosphomimetic mutation of Thr-592. J Biol Chem 290:26352–26359

Wang C, Zhang K, Meng L, Zhang X, Song Y, Zhang Y, Gai Y, Zhang Y, Yu B, Wu J, Wang S, Yu X (2020) The C-terminal domain of feline and bovine SAMHD1 proteins has a crucial role in lentiviral restriction. J Biol Chem 295:4252–4264

Wang F, St Gelais C, de Silva S, Zhang H, Geng Y, Shepard C, Kim B, Yount JS, Wu L (2016) Phosphorylation of mouse SAMHD1 regulates its restriction of human immunodeficiency virus type 1 infection, but not murine leukemia virus infection. Virology 487:273–284

Wei W, Guo H, Gao Q, Markham R, Yu XF (2014) Variation of two primate lineage-specific residues in human SAMHD1 confers resistance to N terminus-targeted SIV Vpx proteins. J Virol 88:583–591

Wei W, Guo H, Han X, Liu X, Zhou X, Zhang W, Yu XF (2012) A novel DCAF1-binding motif required for Vpx-mediated degradation of nuclear SAMHD1 and Vpr-induced G2 arrest. Cell Microbiol 14:1745–1756

Welbourn S, Strebel K (2016) Low dNTP levels are necessary but may not be sufficient for lentiviral restriction by SAMHD1. Virology 488:271–277

White TE, Brandariz-Nunez A, Martinez-Lopez A, Knowlton C, Lenzi G, Kim B, Ivanov D, Diaz-Griffero F (2017) A SAMHD1 mutation associated with Aicardi-Goutieres syndrome uncouples the ability of SAMHD1 to restrict HIV-1 from its ability to downmodulate type I interferon in humans. Hum Mutat 38:658–668

White TE, Brandariz-Nunez A, Valle-Casuso JC, Amie S, Nguyen L, Kim B, Brojatsch J, Diaz-Griffero F (2013a) Contribution of SAM and HD domains to retroviral restriction mediated by human SAMHD1. Virology 436:81–90

White TE, Brandariz-Nunez A, Valle-Casuso JC, Amie S, Nguyen LA, Kim B, Tuzova M, Diaz-Griffero F (2013b) The retroviral restriction ability of SAMHD1, but not its deoxynucleotide triphosphohydrolase activity, is regulated by phosphorylation. Cell Host Microbe 13:441–451

Yan J, Hao C, DeLucia M, Swanson S, Florens L, Washburn MP, Ahn J, Skowronski J (2015) CyclinA2-cyclin-dependent kinase regulates SAMHD1 protein phosphohydrolase domain. J Biol Chem 290:13279–13292

Zhang R, Bloch N, Nguyen LA, Kim B, Landau NR (2014) SAMHD1 restricts HIV-1 replication and regulates interferon production in mouse myeloid cells. PLoS ONE 9:e89558

Zhu CF, Wei W, Peng X, Dong YH, Gong Y, Yu XF (2015) The mechanism of substrate-controlled allosteric regulation of SAMHD1 activated by GTP. Acta Crystallogr D Biol Crystallogr 71:516–524